Journal of Sound and Vibration 328 (2009) 586–606

Contents lists available at ScienceDirect

Journal of Sound and Vibration

journal homepage: www.elsevier.com/locate/jsvi

A contribution to the exact modal solution of in-plane beam structures

C.A.N. Dias *, M. Alves

Group of Solid Mechanics and Structural Impact, Department of Mechatronics and Mechanical Systems Engineering, University of São Paulo, São Paulo 05508-900, Brazil

ARTICLE INFO

Article history:
Received 25 August 2008
Received in revised form
14 August 2009
Accepted 19 August 2009
Handling Editor: C.L. Morfey
Available online 19 September 2009

ABSTRACT

The exact vibration modes and natural frequencies of planar structures and mechanisms, comprised Euler–Bernoulli beams, are obtained by solving a transcendental, non-linear, eigenvalue problem stated by the dynamic stiffness matrix (DSM). To solve this kind of problem, the most employed technique is the Wittrick–Williams algorithm, developed in the early seventies. By formulating a new type of eigenvalue problem, which preserves the internal degrees-of-freedom for all members in the model, the present study offers an alternative to the use of this algorithm. The new proposed eigenvalue problem presents no poles, so the roots of the problem can be found by any suitable iterative numerical method. By avoiding a standard formulation for the DSM, the local mode shapes are directly calculated and any extension to the beam theory can be easily incorporated. It is shown that the method here adopted leads to exact solutions, as confirmed by various examples. Extensions of the formulation are also given, where rotary inertia, end release, skewed edges and rigid offsets are all included.

1. Introduction

A wide range of practical and advanced structures are made by assembling beams. These skeletal structures require very often a dynamic analysis to determine their natural frequencies and vibration modes. This is usually performed using the finite element method, FEM, which requires a large number of elements when high order natural frequencies are sought. Analytical solutions for Euler–Bernouli beam vibration are available though and are not dependent on the domain partitioning. Hence, it is possible to determine natural frequencies and modes of vibrations of structures comprised beams solely by analytical methods. But this is a difficult task since the associated eigenvalue problem, which uses the so-called (exact) dynamic stiffness matrix, DSM, is non-linear and transcendental.

Wittrick and Williams [1] were the ones who developed what seems to be a unique algorithm [2–11] to extract the eigenvalues and modes of the DSM. The W–W algorithm detects the number of natural frequencies below a given cut-off frequency, similar to the Sturm sequence in linear eigenvalue problems [11]. By knowing the number of frequencies, successive applications of the W–W algorithm lead to a range of frequencies in which the natural ones lie. A standard method, as the bi-section, is then used to obtain accurate values for the natural frequencies. The natural vibration modes are calculated independently afterwards, with the additional problem of obtaining the local modes, i.e. the individual vibration of each structural element [9].

* Corresponding author.
E-mail address: candias@usp.br (C.A.N. Dias).

0022-460X/$ - see front matter © 2008 Elsevier Ltd. All rights reserved.
doi:10.1016/j.jsv.2009.08.021

As a consequence of the exact eigenvalue problem, there will be a finite number of global degrees of freedom, DOF, corresponding to the model nodes. There will also be an infinite local DOFs representing the internal displacements of each individual element. The usual way to obtain the DSM is to eliminate the local DOFs, leaving the problem based only on the displacement of the model nodes [2–6]. This leads, however, to some difficulties. First of all, the determinant of the DSM has zeros associated only with the natural frequencies where nodal displacements are at play. It presents poles in the natural frequencies where there is no nodal displacement, leaving local modes with internal displacements. As a characteristic of this numerical problem, the local natural modes cannot be obtained directly from the equilibrium equations yielded by the DSM.

It is worth noting that the presence of poles refrains one of using common algorithms to extract the roots of the frequency equation. This leads to the nearly compulsory use of the W–W algorithm and the inherited difficulty in obtaining the local modes [9,12–14].

Bearing in mind these remarks, the key point of this work is to formulate the eigenvalue problem of a beam-like structure without the elimination of the internal DOF. Instead, we work with a vector that contains the nodal DOF as well as the integration constants of the analytical solution of each beam member. By so proceeding, the two major difficulties commented above are overcome since the posed problem presents no poles. This allows the use of simpler algorithms to extract the roots of the frequency equation. Also, the local modes are directly calculated from the dynamic equilibrium.

In considering the general character and flexibility of this new formulation for the eigenvalue problem, it is somewhat easier to add distributed rotatory inertia for the elements, local concentrated masses and stiffeners. Likewise, it is possible to implement rigid offset, end releases and to prescribe null displacements in directions other than the global ones, as it will be shown. These aspects of dynamic analysis of skeletal structures are difficult to be taken into consideration using the traditional DSM with the W–W algorithm [2,3,6,7]. More recently, Refs. [15–17] defined a new dynamic stiffness matrix, called K_∞, which eliminates the poles from the associated eigenvalue problem. However, this method requires further development in order to include rigid off-set and end release in its formulation.

In the three following sections, the basic equations of the dynamic eigenvalue problem are presented. Next, we provide a few examples where the various features of the present formulation are explored, always comparing the exact results with the ones obtained via FEM. Different features of the problem are covered in the Appendices, with rotatory inertia, end release, skewed edges and rigid offset being developed in the framework of the present formulation.

2. Basic equations

We now present the formulation adopted in this work. We consider Euler–Bernouli beam elements which, assembled in any number in a plane, form a structure. Generally speaking, a computer programme to handle such beam elements has the same characteristics as the one found in a FEM programme. The FEM adopts shape functions to represent the internal element displacements. In our method we use the exact dynamic equilibrium equation so stiffness and mass are exactly taken into account and no mesh refinement is necessary.

The method requires six extra unknowns per element, apart from the joint displacements, i.e. the integration constants. This extra computational effort is well compensated by the use of rather few elements when compared to the number required by the FEM.

Now consider the beam in Fig. 1 with a prismatic and constant cross-section, A, moment of inertia, I, and made of a single isotropic linear elastic material with elastic modulus, E. It can be shown [18], by solving the axial and transverse dynamic governing equation, that the axial, u, and transverse, v, vibration of a beam element i in free vibration are given by

$$u_i(x,t) = [A_i \sin(\beta_i x) + B_i \cos(\beta_i x)]\sin(\omega t) \tag{1}$$

and

$$v_i(x,t) = [C_i \sin(\overline{\beta}_i x) + D_i \cos(\overline{\beta}_i x) + E_i \sinh(\overline{\beta}_i x) + F_i \cosh(\overline{\beta}_i x)]\sin(\omega t). \tag{2}$$

The displacements and the forces at the end of a typical element i for the local coordinate system, Fig. 1, are given, respectively, by

$$\mathbf{Q}_i(t) = \{q_1(t), q_2(t), \ldots, q_6(t)\}^{\mathrm{T}} \tag{3}$$

and

$$\mathbf{P}_i(t) = \{p_1(t), p_2(t), \ldots, p_6(t)\}^{\mathrm{T}}, \tag{4}$$

with the integration constants given by the vector

$$\mathbf{G}_i = \{A_i, B_i, C_i, D_i, E_i, F_i\}^{\mathrm{T}}. \tag{5}$$

Considering now the Euler–Bernouli beam theory, normal force, cross-section rotation, bending moment and shear force can be related to the displacements u_i and v_i. This allows the above displacement and force vectors to be written as

$$\mathbf{Q}_i(t) = \boldsymbol{\phi}_{\mathbf{Qi}} \mathbf{G}_i \sin(\omega t) \tag{6}$$

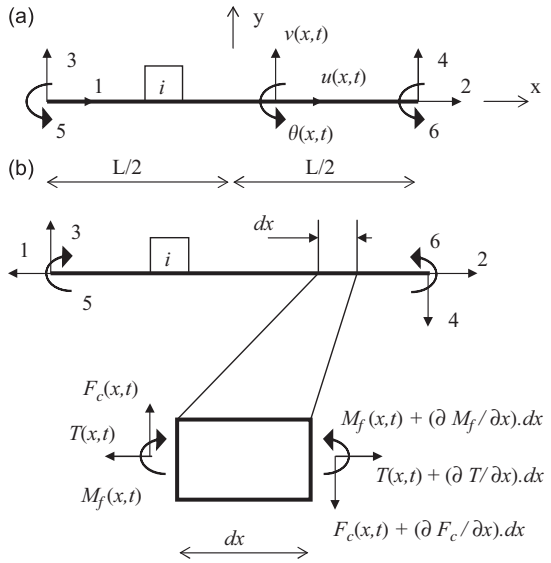

Fig. 1. A beam element. Internal and end (a) displacements and (b) forces.

and

$$\mathbf{P}_i(t) = \boldsymbol{\phi}_{\mathbf{Pi}}\mathbf{G}_i\sin(\omega t), \tag{7}$$

with

$$\boldsymbol{\phi}_{\mathbf{Q}_i} = \begin{bmatrix} -\sin(\lambda_i) & \cos(\lambda_i) & 0 & 0 & 0 & 0 \\ \sin(\lambda_i) & \cos(\lambda_i) & 0 & 0 & 0 & 0 \\ 0 & 0 & -\sin(\overline{\lambda}_i) & \cos(\overline{\lambda}_i) & -\sinh(\overline{\lambda}_i) & \cosh(\overline{\lambda}_i) \\ 0 & 0 & \sin(\overline{\lambda}_i) & \cos(\overline{\lambda}_i) & \sinh(\overline{\lambda}_i) & \cosh(\overline{\lambda}_i) \\ 0 & 0 & \overline{\beta}_i\cos(\overline{\lambda}_i) & \overline{\beta}_i\sin(\overline{\lambda}_i) & \overline{\beta}_i\cosh(\overline{\lambda}_i) & -\overline{\beta}_i\sinh(\overline{\lambda}_i) \\ 0 & 0 & \overline{\beta}_i\cos(\overline{\lambda}_i) & -\overline{\beta}_i\sin(\overline{\lambda}_i) & \overline{\beta}_i\cosh(\overline{\lambda}_i) & \overline{\beta}_i\sinh(\overline{\lambda}_i) \end{bmatrix} \tag{8}$$

and

$$\boldsymbol{\phi}_{\mathbf{P}_i} = \begin{bmatrix} \gamma_i\cos(\lambda_i) & \gamma_i\sin(\lambda_i) & 0 & 0 & 0 & 0 \\ \gamma_i\cos(\lambda_i) & -\gamma_i\sin(\lambda_i) & 0 & 0 & 0 & 0 \\ 0 & 0 & -\overline{\beta}_i\overline{\gamma}_i\cos(\overline{\lambda}_i) & -\overline{\beta}_i\overline{\gamma}_i\sin(\overline{\lambda}_i) & \overline{\beta}_i\overline{\gamma}_i\cosh(\overline{\lambda}_i) & -\overline{\beta}_i\overline{\gamma}_i\sinh(\overline{\lambda}_i) \\ 0 & 0 & -\overline{\beta}_i\overline{\gamma}_i\cos(\overline{\lambda}_i) & \overline{\beta}_i\overline{\gamma}_i\sin(\overline{\lambda}_i) & \overline{\beta}_i\overline{\gamma}_i\cosh(\overline{\lambda}_i) & -\overline{\beta}_i\overline{\gamma}_i\sinh(\overline{\lambda}_i) \\ 0 & 0 & \gamma_i\sin(\overline{\lambda}_i) & -\gamma_i\cos(\overline{\lambda}_i) & -\overline{\gamma}_i\sinh(\overline{\lambda}_i) & \overline{\gamma}_i\cosh(\overline{\lambda}_i) \\ 0 & 0 & -\gamma_i\sin(\overline{\lambda}_i) & \gamma_i\cos(\overline{\lambda}_i) & -\overline{\gamma}_i\sinh(\overline{\lambda}_i) & \overline{\gamma}_i\cosh(\overline{\lambda}_i) \end{bmatrix}, \tag{9}$$

where

$$\lambda_i = \beta_i L_i/2, \quad \overline{\lambda}_i = \overline{\beta}_i L_i/2 \tag{10}$$

and

$$\gamma_i = \beta_i EA_i, \quad \overline{\gamma}_i = \overline{\beta}_i^2 EI_i. \tag{11}$$

The vibration frequency is related to the beam properties and displacement parameters by

$$\omega^2 = \beta_i^2(EA_i/m_i) = \overline{\beta}_i^4(EI_i/m_i), \quad \forall i, \tag{12}$$

when disregarding rotatory inertia influence on the beam dynamics. For higher frequencies, this effect may be important and Appendix A presents a more complete derivation.

2.1. Dynamic stiffness matrix

From Eqs. (6) and (7), a force–displacement relation for the beam element i in local coordinates can be established at once as

$$\mathbf{P}_i(t) = \mathbf{K}_{\mathbf{D_i}}\mathbf{Q}_i(t), \tag{13}$$

where

$$\mathbf{K}_{D_i} = [\boldsymbol{\phi}_{\mathbf{P}_i}\boldsymbol{\phi}_{\mathbf{Q}_i}^{-1}] \tag{14}$$

is the dynamic stiffness matrix for the element i.

2.2. From local to global coordinate systems

Fig. 2 suggests that it is necessary to convert the local degree-of-freedom of the various elements to the global coordinates. Accordingly, the end displacements, $\mathbf{Q}$, and forces, $\mathbf{P}$, are transformed according to

$$\mathbf{Q}_i^*(t) = \mathbf{R}_{\mathbf{Q}_i}(\alpha_i)\mathbf{Q}_\mathbf{i}(t) \tag{15}$$

and

$$\mathbf{P}_i^*(t) = \mathbf{R}_{\mathbf{P}_i}(\alpha_i)\mathbf{P}_i(t), \tag{16}$$

where $\mathbf{R}_{\mathbf{Q}_i}(\alpha_i)$ and $\mathbf{R}_{\mathbf{P}_i}(\alpha_i)$ are well known transformation matrices relating local to global degrees of freedom of an element forming an angle α_i with the global coordinate system.

2.3. Beam elements connectivity

A single end displacement and load vectors, with M elements containing all N degrees-of-freedom of the model, can be assembled as

$$\mathbf{Q}^*(t) = \{\mathbf{Q}_1^*(t), \mathbf{Q}_2^*(t), \ldots, \mathbf{Q}_M^*(t)\}^{\mathrm{T}} \tag{17}$$

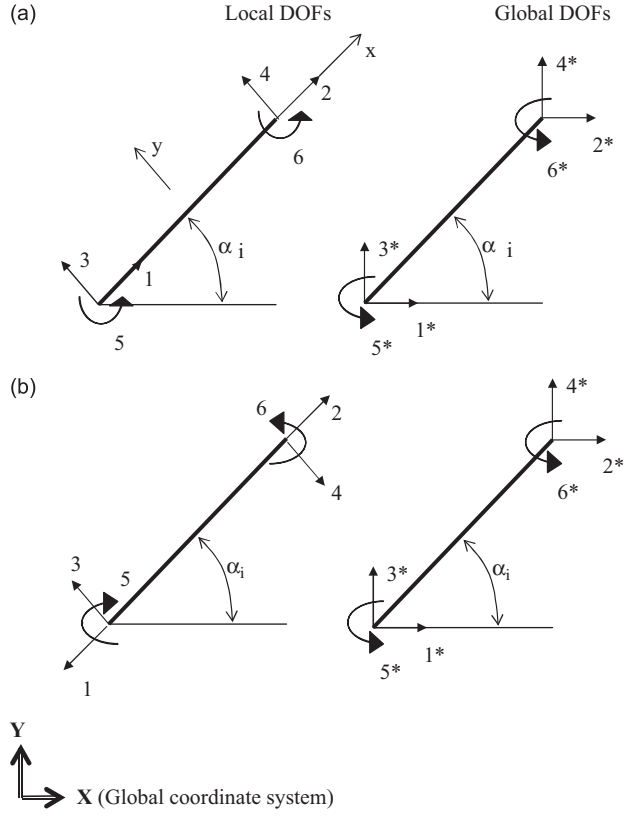

Fig. 2. (a) End displacement and (b) loads conversion to the global coordinate system.

and

$$\mathbf{P}^*(t) = \{\mathbf{P}_1^*(t), \mathbf{P}_2^*(t), \ldots, \mathbf{P}_M^*(t)\}^{\mathrm{T}}, \tag{18}$$

respectively, allowing to establish the relationships

$$\underset{6M\times 1}{\mathbf{Q}^*(t)} = \underset{6M\times N}{\boldsymbol{\psi}_{\mathbf{Q}}}\ \underset{N\times 1}{\overline{\mathbf{Q}}(t)} \tag{19}$$

and

$$\underset{N\times 1}{\overline{\mathbf{P}}(t)} = \underset{N\times 6M}{\boldsymbol{\psi}_{\mathbf{P}}}\ \underset{6M\times 1}{\mathbf{P}^*(t)}, \tag{20}$$

where $\overline{\mathbf{Q}}$ and $\overline{\mathbf{P}}$ are the global node displacement and load vectors, respectively. The matrices $\boldsymbol{\psi}_{\mathbf{Q}}$ and $\boldsymbol{\psi}_{\mathbf{P}}$ are obtained from the connectivity matrix and are formed only by zeroes and ones.

It should be noted that, from $\mathbf{P}^*$, $\overline{\mathbf{P}}$ follows from the nodes equilibrium. Also, it can be shown that

$$\boldsymbol{\psi}_{\mathbf{P}} = \boldsymbol{\psi}_{\mathbf{Q}}^{\mathrm{T}}. \tag{21}$$

2.4. Nodal displacements and loads

Considering the assembled beam structure with N degrees-of-freedom, the global displacements and loads can be written as

$$\overline{\mathbf{Q}}(t) = \{\overline{q}_1(t), \overline{q}_2(t), \ldots, \overline{q}_N(t)\}^{\mathrm{T}} \tag{22}$$

and

$$\overline{\mathbf{P}}(t) = \{\overline{p}_1(t), \overline{p}_2(t), \ldots, \overline{p}_N(t)\}^{\mathrm{T}}. \tag{23}$$

Now, in the case of free vibration, motion is opposed only by the actions of the concentrated mass and concentrated stiffness in each node so that

$$\overline{\mathbf{P}}(t) = -\boldsymbol{\Omega}(\omega)\overline{\mathbf{Q}}(t). \tag{24}$$

Here, $\Omega(\omega)$ can be obtained by considering that in a node n it may occur a translational spring, k_n, acting in a direction γ_n, measured in relation to the global system, X, a rotational spring, k_n^z, in the global axis Z, two translational masses, m_n^x and m_n^y with degrees of freedom in the global directions X and Y, respectively, and a rotational mass, m_n^z, in the global direction Z. Similar to FEM formulation, it can be shown that

$$\underset{N\times N}{\boldsymbol{\Omega}}(\omega) = \mathrm{diag}[(\mathbf{K}_n - \omega^2\mathbf{M}_n)]_{n=1,2,\ldots,N_0}, \tag{25}$$

where N_0 is the number of nodes and

$$\mathbf{K}_n = \begin{bmatrix} k_n\cos^2\gamma_n & k_n\sin\gamma_n\cos\gamma_n & 0 \\ k_n\sin\gamma_n\cos\gamma_n & k_n\sin^2\gamma_n & 0 \\ 0 & 0 & k_n^z \end{bmatrix}, \tag{26}$$

$$\mathbf{M}_n = \mathrm{diag}[m_n^x,\ m_n^y,\ m_n^z]. \tag{27}$$

We remark that these masses aim to represent any rigid body connected to a node n. More precisely, the centre of gravity of the body must coincide with the node position.

2.5. End displacements and loads

The integration constants present in all the M elements can be assembled in a single vector,

$$\boldsymbol{\Theta} = \{\mathbf{G}_1^{\mathrm{T}}, \mathbf{G}_2^{\mathrm{T}}, \ldots, \mathbf{G}_M^{\mathrm{T}}\}^{\mathrm{T}}. \tag{28}$$

Using Eqs. (6) and (15), the end displacement in global coordinates reads

$$\underset{6M\times 1}{\mathbf{Q}^*(t)} = \underset{6M\times 6M}{\boldsymbol{\Phi}_{\mathbf{Q}}}\ \underset{6M\times 1}{\boldsymbol{\Theta}}\ \sin(\omega t), \tag{29}$$

where

$$\boldsymbol{\Phi}_{\mathbf{Q}} = \mathrm{diag}[\mathbf{R}_{\mathbf{Q}_i}\boldsymbol{\phi}_{\mathbf{Q}_i}]_{i=1,2,\ldots,M}. \tag{30}$$

Likewise, the end load vector in global coordinates can be presented in the compact form

$$\underset{6M\times 1}{\mathbf{P}^*(t)} = \underset{6M\times 6M}{\boldsymbol{\Phi}_{\mathbf{P}}}\ \underset{6M\times 1}{\boldsymbol{\Theta}}\ \sin(\omega t), \tag{31}$$

with

$$\boldsymbol{\Phi}_{\mathbf{P}} = \mathrm{diag}[\mathbf{R}_{\mathbf{P}_i}\boldsymbol{\phi}_{\mathbf{P}_i}]_{i=1,2,\ldots,M}. \tag{32}$$

3. The eigenvalue problem

The nodal displacement vector, $\overline{\mathbf{Q}}(t)$, for an harmonic motion of frequency ω, reads

$$\underset{N\times 1}{\overline{\mathbf{Q}}(t)} = \underset{N\times 1}{\mathbf{Q}_0}\sin(\omega t), \tag{33}$$

which can be substituted in Eqs. (19), (20), (24), (29) and (31) to yield

$$\underset{6M\times 6M}{\boldsymbol{\Phi}_{\mathbf{Q}}}\ \underset{6M\times 1}{\boldsymbol{\Theta}} - \underset{6M\times N}{\boldsymbol{\psi}_{\mathbf{Q}}}\ \underset{N\times 1}{\mathbf{Q}_0} = \underset{6M\times 1}{\mathbf{0}} \tag{34}$$

and

$$\underset{N\times 6M}{\boldsymbol{\psi}_{\mathbf{P}}}\ \underset{6M\times 6M}{\boldsymbol{\Phi}_{\mathbf{P}}}\ \underset{6M\times 1}{\boldsymbol{\Theta}} + \underset{N\times N}{\boldsymbol{\Omega}}\ \underset{N\times 1}{\mathbf{Q}_0} = \underset{N\times 1}{\mathbf{0}}. \tag{35}$$

$\boldsymbol{\Phi}_{\mathbf{Q}}$, $\boldsymbol{\psi}_{\mathbf{Q}}$, $\boldsymbol{\psi}_{\mathbf{P}}$, $\boldsymbol{\Phi}_{\mathbf{P}}$ and $\boldsymbol{\Omega}$ are known matrices and to obtain the unknowns, $\mathbf{Q}_0$, it is only necessary to replace Eq. (34) by Eq. (35), giving

$$\underbrace{\mathbf{K}_D(\omega^2)}_{N\times N}\ \underbrace{\mathbf{Q}_0}_{N\times 1} = \underbrace{\mathbf{0}}_{N\times 1}, \tag{36}$$

where

$$\underbrace{\mathbf{K}_D(\omega^2)}_{N\times N} = \underbrace{\boldsymbol{\Psi}_{\mathbf{P}}}_{N\times 6M}\ \underbrace{\boldsymbol{\Phi}_{\mathbf{P}}(\omega)}_{6M\times 6M}\ \underbrace{\boldsymbol{\Phi}_{\mathbf{Q}}^{-1}(\omega)}_{6M\times 6M}\ \underbrace{\boldsymbol{\psi}_{\mathbf{Q}}}_{6M\times N} + \underbrace{\boldsymbol{\Omega}(\omega^2)}_{N\times N}, \tag{37}$$

being $\mathbf{K}_D$ the so-called global dynamic stiffness matrix.

Existence of non-trivial solutions to Eq. (36) are guaranteed when

$$p(\omega^2) = \det[\mathbf{K}_D(\omega^2)] = 0 \quad \mathbf{Q}_0 \neq \mathbf{0} \quad \text{roots} \tag{38}$$

and

$$p(\omega^2) = \det[\mathbf{K}_D(\omega^2)] \to \infty \quad \mathbf{Q}_0 = \mathbf{0} \quad \text{poles}. \tag{39}$$

It is important to notice that in the finite element method the eigenvalue problem presents itself in the non-transcendental, linear, explicit form

$$[\mathbf{K} - \omega^2\mathbf{M}]\mathbf{Q}_0 = \mathbf{0}, \tag{40}$$

with the condition for the existence of a non-trivial solution given by

$$p(\omega^2) = \det[\mathbf{K} - \omega^2\mathbf{M}] = 0, \tag{41}$$

where the mass, $\mathbf{M}$, and the stiffness, $\mathbf{K}$ matrices have constant coefficients and the eigenvalue $\lambda = \omega^2$ is obtained by solving Eq. (41). Alternatively, an inverse vector iterative procedure applied to Eq. (40) gives the eigenvalues and respective eigenvectors. This procedure, where the eigenvectors and eigenvalues are obtained concomitantly, forms the basis of most of the well established methods, e.g. Lanczos and subspace iteration [19], used in commercial finite element codes. Such methods are only possible because the stiffness and mass properties are decoupled, which is not the case for the DSM.

For the particular case of beam finite elements, the stiffness matrix using cubic displacement interpolation is exact but not the mass matrix. Therefore, it is not possible in FEM to perform an exact modal solution.

On the other hand, for various basic structures, if the eigenvalue problem in Eqs. (36)–(39) can be solved, it is possible to obtain an exact modal solution. However, in this case, it is not possible to use well established numerical methods.

One possibility, employed in the literature at large, consists in obtaining the roots and poles of Eqs. (38) and (39). But this leads to some disadvantages:

(1) in order to obtain the dynamic stiffness matrix in its explicit form, it is necessary to evaluate the inverse of $\boldsymbol{\Phi}_{\mathbf{Q}}$, of order $6M$, which may be computational intensive;

(2) the elimination of the integration constants, $\boldsymbol{\Theta}$, as unknowns of the eigenvalue problem, refrains one of the direct calculation of the local modes ($\mathbf{Q}_0 = \mathbf{0}$, $\boldsymbol{\Theta} \neq \mathbf{0}$);
(3) the fact that $\det[\mathbf{K}_D(\omega^2)]$ has zeros and poles for the natural frequencies [9], refrains one from using most of the established methods for extracting eigenvalues leaving, as the only option, the so called W–W algorithm [1].

In this work, these limitations are circumvented by writing the eigenvalue problem in Eqs. (34) and (35) as

$$\underbrace{\begin{bmatrix} \underset{6M\times 6M}{\boldsymbol{\Phi}_Q(\omega^2)} & \underset{6M\times N}{-\boldsymbol{\psi}_Q} \\ \underset{N\times 6M}{\boldsymbol{\psi}_P(\omega^2)\boldsymbol{\Phi}_P} & \underset{N\times N}{\boldsymbol{\Omega}(\omega^2)} \end{bmatrix}}_{=\boldsymbol{\Psi}(\omega^2)} \underbrace{\begin{Bmatrix} \underset{6M\times 1}{\boldsymbol{\Theta}} \\ \underset{N\times 1}{\mathbf{Q}_0} \end{Bmatrix}}_{(6M+N)\times 1} = \underset{(6M+N)\times 1}{\mathbf{0}}, \tag{42}$$

where one should seek for values of ω so that

$$\det\{\boldsymbol{\Psi}(\omega^2)\} = 0. \tag{43}$$

The above method does not present poles so that the roots of Eq. (43) can be obtained progressively from the smaller to a larger value, as specified by giving a cut-off frequency or a desired number of frequencies. Once a natural frequency is established, one returns to Eq. (42) to obtain the integration constants, $\boldsymbol{\Theta}$, and modal nodal displacements, $\mathbf{Q}_0$, vectors.

It is important to remark that the present method requires to solve an eigenvalue problem of order $6M + N$, instead of one of order N, as when using the finite element method. This apparent drawback is compensate by far when considering that only the natural nodes need to be defined. It is not necessary to refine the mesh, as in FEM, specially when high order frequencies are sought.

4. Numerical procedures

To extract the eigenvalues of the problem stated by Eq. (43), a numerical procedure comprising two steps was established. Considering the examples in Fig. 3, the detection of the peaks caused by the various natural frequencies in the function

$$g(f) = -\log\{|\det[\boldsymbol{\Psi}(\omega^2)]|\}, \tag{44}$$

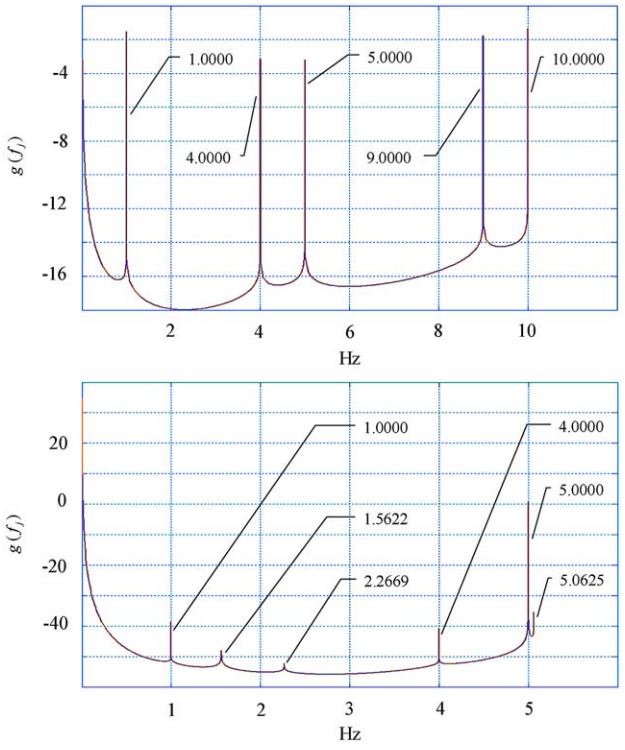

Fig. 3. Searching for the natural frequencies. Cases of Tables 1 (top) and 2 (bottom).

is attained by sweeping it from 0 to a given cut-off frequency, f_{MAX}, at constant intervals Δf, where $f=\omega/2\pi$. When $\det[\mathbf{\Psi}(\omega^2)]$ approaches zero, a peak occurs in the function $g(f)$, which indicates that there is a natural frequency in the interval $[f-\Delta f; f+\Delta f]$. This procedure allows the calculation of both simple and multiple roots of Eq. (43). In the exceptional case where $g(f)$ tends to a very large positive number, i.e. $\det[\mathbf{\Psi}(\omega^2)]\to\infty$, an exact natural frequency value was found.

Differently from the bisection method, the present procedure handles even multiple roots of Eq. (43). However, it does not allow the calculation of the root multiplicity. Hence, it is necessary for another algorithm to find all the natural frequencies below a given cut-off frequency. The W–W algorithm could also be used if it were not for the difficulties it presents in handling the configurations with rigid off-set and end-release explored here. As for the sweeping method, it is very much time consuming, particularly when the first natural frequency is high. This is so because the method requires small frequency steps.

Once all the intervals of natural frequencies in the range $[0-f_{MAX}]$ are determined, a next step is necessary in order to narrow the interval $[f-\Delta f; f+\Delta f]$ using the secant method [19] with a small error tolerance, typically $tolp=10^{-d}$, with $d=16$. Accordingly, defining p_m as the peak frequency found from the analysis of the function $g(f)$ and using

$$f_{1m}^{(0)}=p_m-\Delta f/2 \quad \text{and} \quad f_{2m}^{(0)}=p_m+\Delta f/2 \tag{45}$$

as departure values, very accurate values for the natural frequency can be obtained by

$$f_{nm}^{(k)}=f_{2m}^{(k-1)}-\frac{f_{2m}^{(k-1)}-f_{1m}^{(k-1)}}{1-\dfrac{\det\{\mathbf{\Psi}[(2\pi f_{1m}^{(k-1)})^2]\}}{\det\{\mathbf{\Psi}[(2\pi f_{2m}^{(k-1)})^2]\}}}, \tag{46}$$

with the iterations k being stopped when the difference between the current and previous value of f_{nm} fulfils the chosen tolerance.

Once the natural frequencies are known, the correspondent eigenmode, i.e. the natural vibration mode, can be obtained by linearising the eigenvalue problem. Thus, for each natural frequency, f_i(Hz), one can define

$$\lambda_{1i}=(f_i/2\pi)^2(1-tolp), \tag{47}$$

$$\lambda_{2i}=(f_i/2\pi)^2(1+tolp), \tag{48}$$

$$\mathbf{\Psi}_i^M=[\mathbf{\Psi}(\lambda_{1i})-\mathbf{\Psi}(\lambda_{2i})]/(\lambda_{2i}-\lambda_{1i}) \tag{49}$$

and

$$\mathbf{\Psi}_i^K=\mathbf{\Psi}(\lambda_{1i})+\lambda_{1i}\mathbf{\Psi}_i^M, \tag{50}$$

with $\lambda=\omega^2$.

To obtain the mode i, it is only necessary to solve the linear eigenvalue problem

$$[\mathbf{\Psi}_i^K-\lambda\mathbf{\Psi}_i^M]\begin{Bmatrix}\mathbf{\Theta}_i\\ \mathbf{Q}_{0_i}\end{Bmatrix}=\mathbf{0}, \tag{51}$$

which will yield both the nodal displacement vector, $\mathbf{Q}_{0_i}$, and the integration constants vector, $\mathbf{\Theta}_i$, from which the internal displacements of each element is determined.

It is remarked that the eigenvalue problem in Eq. (51) can be solved by any appropriate method used for linear problems. Also, it has a finite number of solutions; among them, one should take only the one whose natural frequency, f_i, is the closest to f_i. A tolerance between f_i and f_i of $10^{-d/2}$ is recommended.

5. Examples and discussion

The numerical procedure described before was implemented in the code VIGENE [20] using the MATLAB platform. The programme has some features which allow the analysis of any plane structure made of beams, whose nodes may have springs and concentrated masses. Skewed supports, end release and rigid off-sets are also considered, as detailed in the Appendices.

The first two examples here are simple enough to allow a comparison of the present formulation with analytical solutions. Other more involved examples are compared only with FEM solutions using the software ANSYS.

Table 1 shows the results for a simply supported beam, with the properties given in the caption. As expected from the present method, the results given by the programme VIGENE are mesh independent and exact, in contradistinction with the FEM results.

Let us now consider the simply supported square frame in Fig. 4 with the properties listed in Table 2. It is clear from the results in Table 2 that the methodology described here is capable of matching the analytical solution, which is approached

Table 1
Natural frequencies (Hz) for a simply supported beam with no axial translation of the supports.

Num. of elem.	Mode Type $i=$	1 Bending 1	2 Bending 2	3 Axial 1	4 Bending 3	5 Axial 2
1	VIGENE	1.0000	4.0000	5.0000	9.0000	10.000
	FEM	–	–	–	–	–
10	VIGENE	1.0000	4.0000	5.0000	9.0000	10.000
	FEM	0.9999	3.9995	4.9795	8.9939	9.8363
100	VIGENE	1.0000	4.0000	5.0000	9.0000	10.000
	FEM	1.0000	4.0000	4.9998	9.0000	9.9984
	Analytical	1.0000	4.0000	5.0000	9.0000	10.000

$L=10$, $EA=\pi^2 10^4$, $EI=4\times10^4$, $m=\pi^2$. Analytical solution for the ith mode: Axial $\rightarrow f_i=(i/2)\sqrt{EA/mL^2}=5i$, Bending $\rightarrow f_i=(\pi i^2/2)\sqrt{EI/mL^4}=i^2$. The FEM analysis was performed in ANSYS using lumped mass and no rotatory inertia.

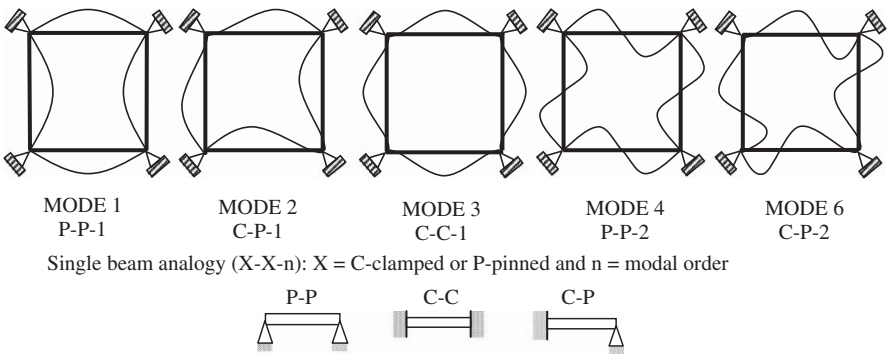

Fig. 4. Mode shapes for the square frame in Table 2. Analytical solution based on single beam analogy applied to a single edge.

Table 2
Natural frequencies (Hz) for a simply supported frame (single beam analogy).

Mode	Roots multiplicity	b.c.	Mode	Type	Analyt.	FEM	VIGENE	$\mathbf{Q}_0$
1	1	S–S	1	Lateral	1.0000	1.0000	1.0000	$\neq\mathbf{0}$
2	2	C–S	1	Lateral	1.5622	1.5622	1.5622	$\neq\mathbf{0}$
3	1	C–C	1	Lateral	2.2669	2.2669	2.2669	$=\mathbf{0}$
4	1	S–S	2	Lateral	4.0000	4.0000	4.0000	$\neq\mathbf{0}$
5	4	S–S	1	Axial	5.0000	4.9998	5.0000	$=\mathbf{0}$
6	2	C–S	2	Lateral	5.0625	5.0625	5.0625	$\neq\mathbf{0}$

All four members with the same properties as in Table 1. The FEM analysis was performed in ANSYS with no rotatory inertia and 100 elements per side. The VIGENE solutions, also with no rotatory inertia effects, uses only 1 element per side.

by the FEM results only when mesh refinement of 100 finite elements is considered. It is emphasised with this example that our method detects multiple roots as well as local modes for which there is no nodal displacement ($\mathbf{Q}_0=\mathbf{0}$).

The square frame in Fig. 4 has its all four corners simply supported so only rotations are allowed. Hence, analytical solutions can be obtained directly from the beam theory when considering a combination of simply supported and clamped cases. For example, the first and second natural frequencies of the frame in the figure corresponds to the lateral vibration of a beam simply supported in both sides and a beam simply supported in one side and clamped in the other, respectively.

Let us now consider the six global DOF structure in Fig. 5. The results of the analysis listed in Table 3 show that only a high mesh density allows the FEM method to approach the exact solution by VIGENE.

Finally, we analyse a two storey building where lateral flexible constraints and concentrated masses are considered, Fig. 6. The results in Table 4 again clearly indicate the good performance of the VIGENE method. Also, these results explore the influence of rotatory inertia, as theoretically explained in the Appendices.

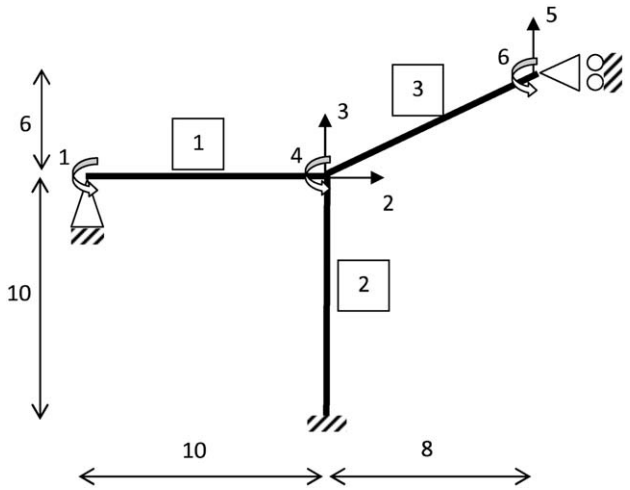

Fig. 5. Geometry of a frame.

Table 3
Natural frequencies (Hz) for the structure in Fig. 5.

Nodes	Mode	1	2	3	4	5
4	VIGENE	0.89113	1.1256	1.3211	2.0395	2.3711
4	FEM	0.85010	N/A	1.3220	2.1349	N/A
31	FEM	0.89156	1.1253	1.3179	2.0373	2.3703
301	FEM	0.89114	1.1256	1.3211	2.0395	2.3711

All members with the same properties as in Table 1. No rotatory inertia neither in VIGENE nor in the FEM analysis, which employs lumped mass matrix.

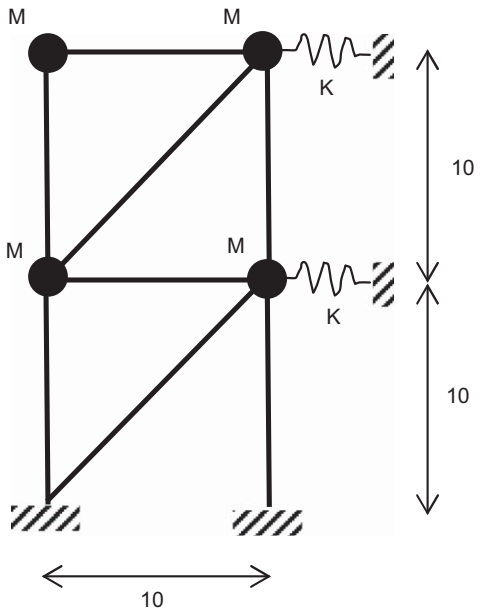

Fig. 6. A two-storey building model with lateral flexible constraints.

Table 4
Natural frequencies (Hz) for the building model with the dimensions in Fig. 6 and members properties, other than length, as in Table 1.

Case	Rotat. inertia	Num. nodes	mode→	1	2	3	4	5
$M=0$, $K=0$	No	6	VIGENE	0.25487	0.72793	0.81989	0.97207	1.1196
		798	FEM[a]	0.25487	0.72792	0.81989	0.97206	1.1196
	Yes	6	VIGENE	0.25480	0.72526	0.81584	0.96253	1.1046
		798	FEM[b]	0.25464	0.72526	0.81551	0.96152	1.1036
$M=100$, $K=0$	No	6	VIGENE	0.19479	0.57468	0.65871	0.91720	0.98390
		798	FEM[a]	0.19479	0.57468	0.65871	0.91720	0.98389
	Yes	6	VIGENE	0.19477	0.57371	0.65757	0.90995	0.97537
		798	FEM[b]	0.19468	0.57329	0.65771	0.91012	0.97451
$M=100$, $K=5000$	No	6	VIGENE	0.49052	0.62485	0.72733	0.92874	0.99244
		798	FEM[a]	0.49052	0.62485	0.72732	0.92874	0.99243
	Yes	6	VIGENE	0.49006	0.62416	0.72603	0.92002	0.98403
		798	FEM[b]	0.49019	0.62427	0.72516	0.92038	0.98316

[a] ANSYS with lumped mass matrix and no rotatory inertia.
[b] ANSYS with consistent mass matrix and rotatory inertia.

6. Conclusion

In this article, an alternative to the W–W algorithm was developed in order to solve the eigenvalue problem related to frame structure vibration calculation. It is shown in detail in the Appendices how some special effects can be included in a more general formulation. A new definition for the DSM is proposed which yields no poles in its determinant. This allows one to use an algorithm which does not require, differently from the W–W algorithm, the knowledge of the clamped–clamped natural frequencies for all members in the model, which is particulary difficult in the presence of rigid offset and end release.

As an additional advantage, the present formulation preserves an accurate representation of the mode shapes by working directly with the integration constants of each element of the entire model. Hence, in a further evaluation of forced response of a structure, it is possible an accurate calculation of the dynamic stress levels.

Appendix A. Rotatory inertia

Rotatory inertia, κ, can be considered by solving the equilibrium equation

$$m\ddot{v}(x,t)+EI\partial^4 v(x,t)/\partial x^4-\kappa\partial^2\ddot{v}(x,t)/\partial x^2=0, \tag{A.1}$$

whose solution is

$$v(x,t)=[C\sin(\beta_T x)+D\cos(\beta_T x)+E\sinh(\beta_H x)+F\cosh(\beta_H x)]\sin(\omega t), \tag{A.2}$$

where now the β coefficients are different for the trigonometric and hyperbolic functions.

Substituting Eq. (A.2) into Eq. (A.1) gives

$$\omega^2=\frac{\beta_T^4 EI}{m+\kappa\beta_T^2}=\frac{\beta_H^4 EI}{m-\kappa\beta_H^2}, \tag{A.3}$$

or

$$\beta_T^2=(1/2)[+\omega^2\kappa/EI+\sqrt{\Delta}] \tag{A.4}$$

and

$$\beta_H^2=(1/2)[-\omega^2\kappa/EI+\sqrt{\Delta}], \tag{A.5}$$

with

$$\Delta=[\omega^2(\kappa/EI)]^2+4[\omega^2(m/EI)]>0. \tag{A.6}$$

Bearing in mind Eqs. (8) and (9), the terms related to the trigonometric functions become now $\overline{\beta}=\beta_T$ and $\overline{\lambda}=\beta_T L/2$, whereas the ones related to the hyperbolic functions are now $\overline{\beta}=\beta_H$ and $\overline{\lambda}=\beta_H L/2$. Note that, if $\kappa=0$, the no rotatory case is recovered, i.e. $\beta_T=\beta_H=\overline{\beta}$ and $\lambda_T=\lambda_H=\overline{\lambda}$.

As a general rule, rotatory inertia does not affect the low order natural frequencies of slender beams. For short beams or for high natural frequencies, the effect can be significant. This can be seen in Table 3, where in the first mode the error is around 0.03 percent, while for the fifth mode this errors increase to almost 1.4 percent. Transverse shear effects are also

important for short beams or high order modes but the present formulation has not been yet extended to the Timoshenko beam theory.

Appendix B. End release

B.1. Relationship between forces and integration constants

To relax the loads in the element end, consider Eq. (7), with index i dropped for the sake of simplicity,

$$\underset{\mathbf{6\times1}}{\mathbf{P}} = \underset{\mathbf{6\times6}}{\boldsymbol{\phi}_P}\,\underset{\mathbf{6\times1}}{\mathbf{G}}. \tag{B.1}$$

This equation can be partitioned according to

$$\begin{Bmatrix} \underset{na\times1}{\mathbf{P_a}} \\ \underset{1\times1}{\mathbf{P_b}} \\ \underset{nc\times1}{\mathbf{P_c}} \end{Bmatrix} = \begin{bmatrix} \underset{na\times na}{\boldsymbol{\phi}_{Paa}} & \underset{na\times1}{\boldsymbol{\phi}_{Pab}} & \underset{na\times nc}{\boldsymbol{\phi}_{Pac}} \\ \underset{1\times na}{\boldsymbol{\phi}_{Pba}} & \underset{1\times1}{\boldsymbol{\phi}_{Pbb}} & \underset{1\times nc}{\boldsymbol{\phi}_{Pbc}} \\ \underset{nc\times na}{\boldsymbol{\phi}_{Pca}} & \underset{nc\times1}{\boldsymbol{\phi}_{Pcb}} & \underset{nc\times nc}{\boldsymbol{\phi}_{Pcc}} \end{bmatrix} \begin{Bmatrix} \underset{na\times1}{\mathbf{G_a}} \\ \underset{1\times1}{\mathbf{G_b}} \\ \underset{nc\times1}{\mathbf{G_c}} \end{Bmatrix}, \tag{B.2}$$

with $na+1+nc=6$, from which the following equations follow:

$$\mathbf{P_a} = \boldsymbol{\phi}_{Paa}\mathbf{G}_a + \boldsymbol{\phi}_{Pab}\mathbf{G}_b + \boldsymbol{\phi}_{Pac}\mathbf{G}_c, \tag{B.3}$$

$$\mathbf{P_b} = \boldsymbol{\phi}_{Pba}\mathbf{G}_a + \boldsymbol{\phi}_{Pbb}\mathbf{G}_b + \boldsymbol{\phi}_{Pbc}\mathbf{G}_c \tag{B.4}$$

and

$$\mathbf{P_c} = \boldsymbol{\phi}_{Pca}\mathbf{G}_a + \boldsymbol{\phi}_{Pcb}\mathbf{G}_b + \boldsymbol{\phi}_{Pcc}\mathbf{G}_c. \tag{B.5}$$

Under the relaxation condition $\mathbf{P}_b = 0,\ \forall\mathbf{G}$ and defining $\mu = 1/\boldsymbol{\phi}_{P_{bb}}$, from Eq. (B.4), it follows

$$\mathbf{G}_b = -\mu[\boldsymbol{\phi}_{P_{ba}}\mathbf{G}_a + \boldsymbol{\phi}_{P_{bc}}\mathbf{G}_c], \tag{B.6}$$

which can be substituted in Eq. (B.3) to give

$$\mathbf{P}_a = [\boldsymbol{\phi}_{P_{aa}} - \mu\boldsymbol{\phi}_{P_{ab}}\boldsymbol{\phi}_{P_{ba}}]\mathbf{G}_a + [\boldsymbol{\phi}_{P_{ac}} - \mu\boldsymbol{\phi}_{P_{ab}}\phi P_{bc}]\mathbf{G}_c \tag{B.7}$$

and in Eq. (B.5) to give

$$\mathbf{P}_c = [\boldsymbol{\phi}_{P_{ca}} - \mu\boldsymbol{\phi}_{P_{cb}}\boldsymbol{\phi}_{P_{ba}}]\mathbf{G}_a + [\boldsymbol{\phi}_{P_{cc}} - \mu\boldsymbol{\phi}_{P_{cb}}\boldsymbol{\phi}_{P_{bc}}]\mathbf{G}_c. \tag{B.8}$$

Knowing that $\mathbf{P}_b = 0$, Eq. (B.2) becomes

$$\underset{6\times1}{\mathbf{P}} = \underset{6\times6}{\hat{\boldsymbol{\phi}}_P}\,\underset{6\times1}{\mathbf{C}}, \tag{B.9}$$

where

$$\hat{\boldsymbol{\phi}}_P = \begin{bmatrix} \underset{na\times na}{[\boldsymbol{\phi}_{P_{aa}} - \mu\boldsymbol{\phi}_{P_{ab}}\boldsymbol{\phi}_{P_{ba}}]} & \underset{na\times1}{0} & \underset{na\times nc}{[\boldsymbol{\phi}_{P_{ac}} - \mu\boldsymbol{\phi}_{P_{ab}}\boldsymbol{\phi}_{P_{bc}}]} \\ \underset{1\times na}{0} & \underset{1\times1}{0} & \underset{1\times nc}{0} \\ \underset{nc\times na}{[\boldsymbol{\phi}_{P_{ca}} - \mu\boldsymbol{\phi}_{P_{cb}}\boldsymbol{\phi}_{P_{ba}}]} & \underset{nc\times1}{0} & \underset{nc\times nc}{[\boldsymbol{\phi}_{P_{cc}} - \mu\boldsymbol{\phi}_{P_{cb}}\boldsymbol{\phi}_{P_{bc}}]} \end{bmatrix}. \tag{B.10}$$

B.2. Relationship between displacement and integration constants

In a similar manner, one can obtain the matrix $\boldsymbol{\phi}_Q$ under the effect of the end release as

$$\underset{6\times1}{\mathbf{Q}} = \underset{6\times6}{\hat{\boldsymbol{\phi}}_Q}\,\underset{6\times1}{\mathbf{G}}, \tag{B.11}$$

where

$$\hat{\boldsymbol{\phi}}_Q = \begin{bmatrix} \underset{na\times na}{[\boldsymbol{\phi}_{Q_{aa}} - \mu\boldsymbol{\phi}_{Q_{ab}}\boldsymbol{\phi}_{P_{ba}}]} & \underset{na\times1}{0} & \underset{na\times nc}{[\boldsymbol{\phi}_{Q_{ac}} - \mu\boldsymbol{\phi}_{Q_{ab}}\boldsymbol{\phi}_{P_{bc}}]} \\ \underset{1\times na}{[\boldsymbol{\phi}_{Q_{ba}} - \mu\boldsymbol{\phi}_{Q_{bb}}\boldsymbol{\phi}_{P_{ba}}]} & \underset{1\times1}{0} & \underset{1\times nc}{[\boldsymbol{\phi}_{Q_{bc}} - \mu\boldsymbol{\phi}_{Q_{bb}}\boldsymbol{\phi}_{P_{bc}}]} \\ \underset{nc\times na}{[\boldsymbol{\phi}_{Q_{ca}} - \mu\boldsymbol{\phi}_{Q_{cb}}\boldsymbol{\phi}_{P_{ba}}]} & \underset{nc\times1}{0} & \underset{nc\times nc}{[\boldsymbol{\phi}_{Q_{cc}} - \mu\boldsymbol{\phi}_{Q_{cb}}\boldsymbol{\phi}_{P_{bc}}]} \end{bmatrix}. \tag{B.12}$$

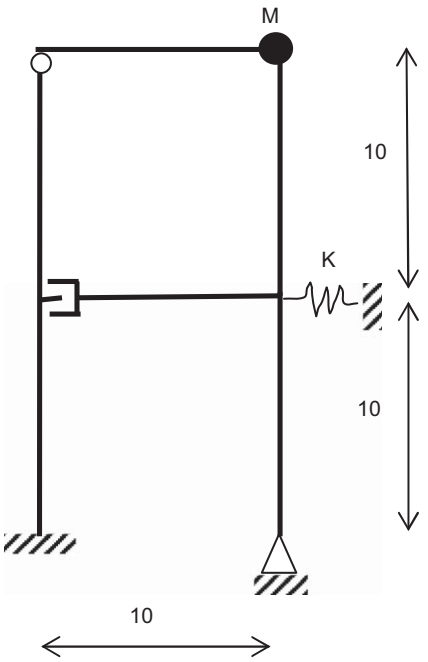

Fig. B1. Released structure. $EA = 40.0E6$, $EI = 12.0E6$, $m = 40$ for the horizontal members, $EA = 100.0E6$, $EI = 4.0E6$, $m = 10$, for the vertical members, $M = 100$, $K = 5.0E4$.

Table B1
Natural frequencies (Hz) for the structure in Fig. B1.

Mode	VIGENE 6 nodes	FEM 600 nodes
1	0.99229	0.99190
2	2.3670	2.3666
3	4.0573	4.0562
4	5.1530	5.1612
5	8.1656	8.1295

VIGENE—with rotatory inertia considered, ANSYS—rotatory inertia considered, consistent mass matrix, finite elements of length 0.1.

B.3. The eigenvalue problem

Substituting $\boldsymbol{\phi}_{Q_i}$ and $\boldsymbol{\phi}_{P_i}$ by $\hat{\boldsymbol{\phi}}_{Q_i}$ and $\hat{\boldsymbol{\phi}}_{P_i}$ in Eqs. (30) and (32), respectively, one obtains the relaxed version of the eigenvalue problem given by Eq. (42). The same numerical procedure presented before can be used, just taking care to eliminate the line and column of the respective relaxed degree of freedom.

B.4. Example

Consider the example in Fig. B1, where the top bending moment on the left end column and the normal force in the first beam floor are relaxed. The results of this analysis are shown in Table B1.

Appendix C. Skewed edges

C.1. Degree of freedom elimination

Nodes are defined in such a way that their translational degrees of freedom are defined in the global cartesian axis. This refrains one from modelling supports whose motion is allowed in directions other than the global axis. To overcome this difficulty, finite element programmes use the so-called constrain equations, where an additional equation relating the DOF

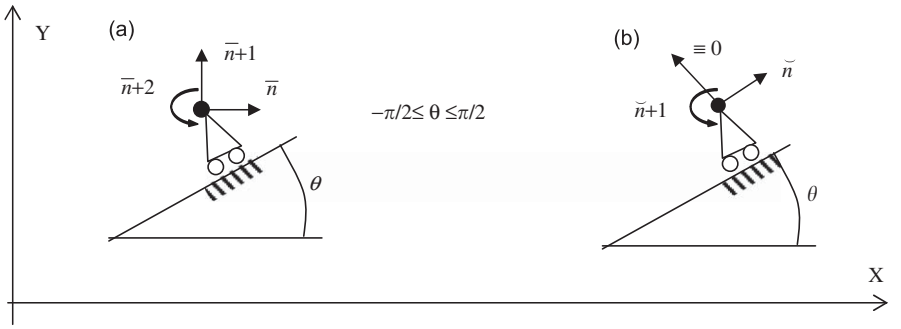

Fig. C1. Skew edges for the simply supported beam case. (a) Global and (b) local degrees of freedom.

is added. The same approach is used here and, from Fig. C1, we may write

$$\overline{\mathbf{Q}}_j(t) = \breve{\mathbf{R}}_j \breve{\mathbf{Q}}_j(t) \Rightarrow \breve{\mathbf{Q}}_j(t) = \breve{\mathbf{R}}_j^{\mathrm{T}} \overline{\mathbf{Q}}_j(t), \tag{C.1}$$

where

$$\overline{\mathbf{Q}}_j(t) = \{\overline{q}_n(t), \overline{q}_{n+1}(t), \overline{q}_{n+2}(t)\}^{\mathrm{T}} \tag{C.2}$$

is the displacement vector of node j before a constrain is applied and

$$\breve{\mathbf{Q}}_j(t) = \{\breve{q}_n(t), 0, \breve{q}_{n+2}(t)\}^{\mathrm{T}} \tag{C.3}$$

is the displacement vector, at the same node, after the imposition of the skew edge condition, so that there is no translation perpendicular to the plane.

Being θ the skew edge angle, the rotation matrix is

$$\breve{\mathbf{R}}_j = \begin{bmatrix} \cos\theta & 0 & 0 \\ \sin\theta & 0 & 0 \\ 0 & 0 & 1 \end{bmatrix} \quad \text{or} \quad \breve{\mathbf{R}}_j = \begin{bmatrix} \cos\theta & 0 \\ \sin\theta & 0 \end{bmatrix} \tag{C.4}$$

for a simply and clamped skew edge support, respectively. In the clamped case, not shown in Fig. C1, the rotational DOF should also be removed.

Now, a model with N degrees of freedom and N_0 nodes has the displacement nodes vector written as

$$\overline{\mathbf{Q}}(t) = \{\overline{q}_1(t), \overline{q}_2(t), \ldots, \overline{q}_N(t)\}^{\mathrm{T}} = \{\overline{\mathbf{Q}}_1(t), \overline{\mathbf{Q}}_2(t), \ldots, \overline{\mathbf{Q}}_{N_0}(t)\}^{\mathrm{T}}, \tag{C.5}$$

or

$$\underset{N\times 1}{\overline{\mathbf{Q}}}(t) = \underset{N\times L}{\boldsymbol{\phi}_N} \underset{L\times 1}{\breve{\mathbf{Q}}}(t), \tag{C.6}$$

where

$$\boldsymbol{\phi}_N = \mathrm{diag}[\breve{\mathbf{R}}_j] \quad \text{for } j = 1, 2, \ldots, N_0, \tag{C.7}$$

with $L < N$ being the total number of degrees of freedom resulting from the elimination of all DOF due to the skewed edges.

The transformation in Eq. (C.6) can be equally applied to the load vector, i.e.

$$\underset{L\times 1}{\breve{\mathbf{P}}}(t) = \underset{L\times N}{\boldsymbol{\phi}_N^{\mathrm{T}}} \underset{N\times 1}{\overline{\mathbf{P}}}(t), \tag{C.8}$$

so that the original eigenvalue problem of Eqs. (34) and (35) changes to

$$\underset{6M\times 6M}{\boldsymbol{\phi}_Q} \underset{6M\times 1}{\boldsymbol{\Theta}} - \underset{6M\times N}{\boldsymbol{\psi}_Q} \underset{N\times L}{\boldsymbol{\phi}_N} \underset{L\times 1}{\breve{\mathbf{Q}}_0} = \underset{6M\times 1}{\mathbf{0}}$$

$$\underset{L\times N}{\boldsymbol{\phi}_N^{\mathrm{T}}} \underset{N\times 6M}{\boldsymbol{\psi}_P} \underset{6M\times 6M}{\boldsymbol{\phi}_P} \underset{6M\times 1}{\boldsymbol{\Theta}} + \underset{L\times N}{\boldsymbol{\phi}_N^{\mathrm{T}}} \underset{N\times N}{\boldsymbol{\Omega}} \underset{N\times L}{\boldsymbol{\phi}_N} \underset{L\times 1}{\breve{\mathbf{Q}}_0} = \underset{L\times 1}{\mathbf{0}}, \tag{C.9}$$

where the same numerical strategy used before for the eigensolution is also valid here.

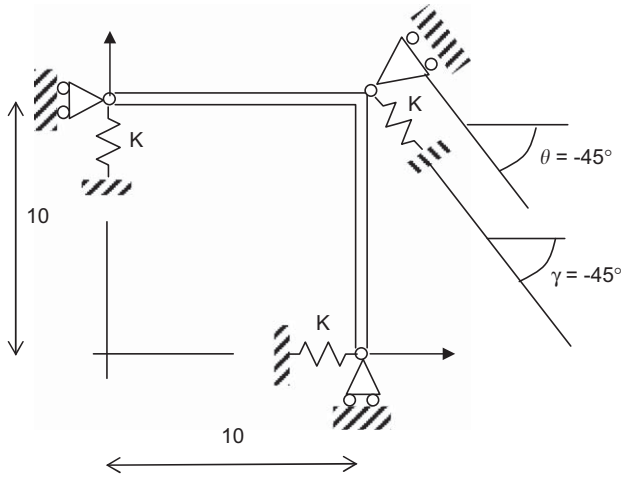

Fig. C2. A structure with a skew edged. Beam properties as in Table 1 and $K = 500$.

Table C1
Natural frequencies (Hz) of the structure in Fig. C2.

Mode	VIGENE 2 elements	FEM 20 elements
1	0.54444	0.54450
2	0.75946	0.75564
3	1.5556	1.5234
4	2.2951	2.2104
5	2.4791	2.4260

VIGENE—rotatory inertia considered, ANSYS—rotatory inertia considered, consistent mass matrix, finite elements of length 0.1.

C.2. Example

The structure in Fig. C2 serves as an example of a simple application of the procedure described in this section, with Table C1 listing the main results, when adopting the same beam properties as in Table 1.

Appendix D. Rigid offsets

Consider the finite element in Fig. D1 of virtual length L_T and stiff ends defined by the dimensions a_I, b_I, a_J and b_J, so that the flexible length can be obtained from

$$L^2 = \sqrt{L_T^2 - (b_I + b_J)^2} - (a_I + a_J) > 0, \tag{D.1}$$

with

$$\alpha = \alpha_T - \arcsin[(b_I + b_J)/L_T]. \tag{D.2}$$

D.1. Relationship between forces and displacements

To consider the stiff ends, Figs. D1 and D2 help in relating the displacements

$$\mathbf{Q}(t) = \{q_1(t), q_2(t), \ldots, q_6(t)\}^{\mathrm{T}} \tag{D.3}$$

and loads

$$\mathbf{P}(t) = \{p_1(t), p_2(t), \ldots, p_6(t)\}^{\mathrm{T}} \tag{D.4}$$

in the exterior points I and J with the corresponding values

$$\hat{\mathbf{Q}}(t) = \{\hat{q}_1(t), \hat{q}_2(t), \ldots, \hat{q}_6(t)\}^{\mathrm{T}} \tag{D.5}$$

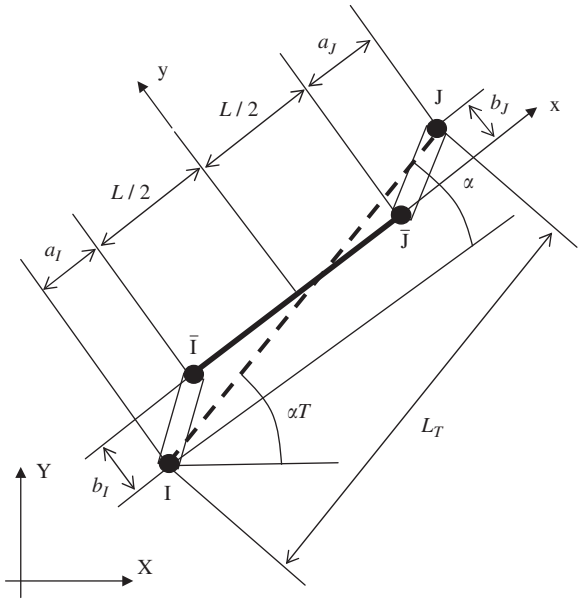

Fig. D1. Beam element with rigid offset.

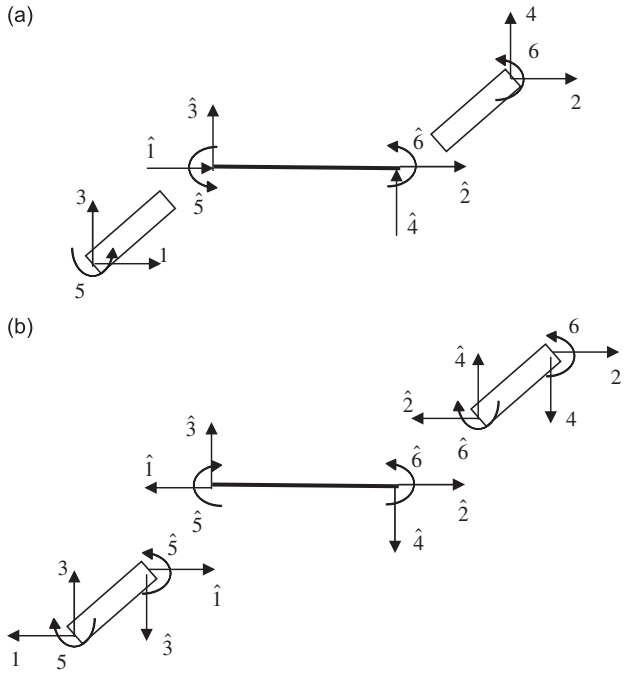

Fig. D2. Numbering of (a) displacement and (b) loads.

and

$$\hat{\mathbf{P}}(t) = \{\hat{p}_1(t), \hat{p}_2(t), \ldots, \hat{p}_6(t)\}^{\mathrm{T}}, \tag{D.6}$$

for the interior points $\bar{I}$ and $\bar{J}$, according to

$$\mathbf{Q}(t) = \mathbf{T}_{\mathrm{Q}}\hat{\mathbf{Q}}(t) = \mathbf{T}_{\mathrm{Q}}\boldsymbol{\phi}_{\mathrm{Q}}\mathbf{G}\sin(\omega t) \tag{D.7}$$

and

$$\mathbf{P}(t) = \mathbf{T}_P\hat{\mathbf{P}}(t) = \mathbf{T}_P\boldsymbol{\phi}_P\mathbf{G}\sin(\omega t), \tag{D.8}$$

where

$$\mathbf{T}_Q = \begin{bmatrix} 1 & 0 & 0 & 0 & +b_I & 0 \\ 0 & 1 & 0 & 0 & 0 & -b_J \\ 0 & 0 & 1 & 0 & -a_I & 0 \\ 0 & 0 & 0 & 1 & 0 & +a_J \\ 0 & 0 & 0 & 0 & 1 & 0 \\ 0 & 0 & 0 & 0 & 0 & 1 \end{bmatrix} \tag{D.9}$$

and

$$\mathbf{T}_P = \begin{bmatrix} 1 & 0 & 0 & 0 & 0 & 0 \\ 0 & 1 & 0 & 0 & 0 & 0 \\ 0 & 0 & 1 & 0 & 0 & 0 \\ 0 & 0 & 0 & 1 & 0 & 0 \\ -b_I & 0 & -a_I & 0 & 1 & 0 \\ 0 & +b_J & 0 & +a_J & 0 & 1 \end{bmatrix}. \tag{D.10}$$

D.2. Inertia of the stiff ends

To consider the inertia of the stiff ends, one should rewrite Eq. (D.8) as

$$\mathbf{P}(t) = [\mathbf{T}_P\boldsymbol{\phi}_P - \omega^2\mathbf{S}_Q\boldsymbol{\phi}_Q]\mathbf{G}\sin(\omega t) \tag{D.11}$$

where

$$\mathbf{S}_Q = \mathbf{HJU}[\mathbf{T}_Q + \mathbf{I}], \tag{D.12}$$

with

$$\mathbf{H} = \begin{bmatrix} -2 & 0 & 0 & 0 & 0 & 0 \\ 0 & 0 & 0 & +2 & 0 & 0 \\ 0 & +2 & 0 & 0 & 0 & 0 \\ 0 & 0 & 0 & 0 & -2 & 0 \\ +b_I & -a_I & -2 & 0 & 0 & 0 \\ 0 & 0 & 0 & +b_J & -a_J & -2 \end{bmatrix} \tag{D.13}$$

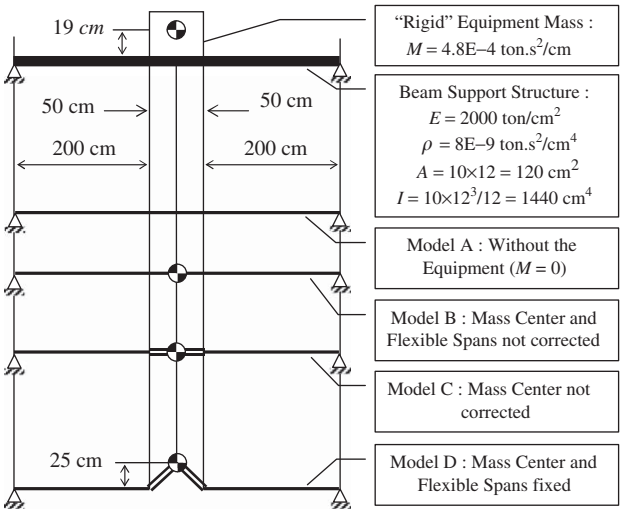

Fig. D3. A simple practical example demonstrating the usefulness of rigid offset.

and

$$\mathbf{U} = \begin{bmatrix} 1/2 & 0 & 0 & 0 & 0 & 0 \\ 0 & 0 & 1/2 & 0 & 0 & 0 \\ 0 & 0 & 0 & 0 & 1/2 & 0 \\ 0 & 1/2 & 0 & 0 & 0 & 0 \\ 0 & 0 & 0 & 1/2 & 0 & 0 \\ 0 & 0 & 0 & 0 & 0 & 0 \end{bmatrix}, \tag{D.14}$$

index i being omitted.

Here,

$$\mathbf{J} = \text{diag}[\mathbf{M}_{TI},\ \mathbf{M}_{TI},\ \mathbf{M}_{RI},\ \mathbf{M}_{TJ},\ \mathbf{M}_{TJ},\ \mathbf{M}_{RJ}] \tag{D.15}$$

is a matrix that contains all the contributions of translational and rotatory inertia of both stiff ends, taking the respective centres of mass as the reference.

Table D1
Results for the rigid offset case presented in Fig. D3.

Natural frequencies (Hz)								
MODE	Model A		Model B		Model C		Model D	
	VIGENE (1)	Ilanko (2)	VIGENE (1)	Ilanko (2)	VIGENE (1)	Ilanko (2)	VIGENE (1)	FEM (3)
1	10.833	10.833	6.2627	6.2627	9.0552	9.0552	9.0552	9.0542
2	43.531	43.531	43.531	43.531	45.534	45.534	42.253	42.228
3	97.945	97.945	74.858	74.858	115.23	115.23	115.23	115.00
4	174.13	174.13	174.13	174.13	197.55	197.55	164.69	164.30
5	272.07	272.07	228.02	228.02	354.16	354.16	329.59	328.60

(1) VIGENE models with only three nodes and two beams; (2) results from Ilanko [22] using his program "Newtonian.exe"; (3) ANSYS solver with 40 equal finite elements type beam54.

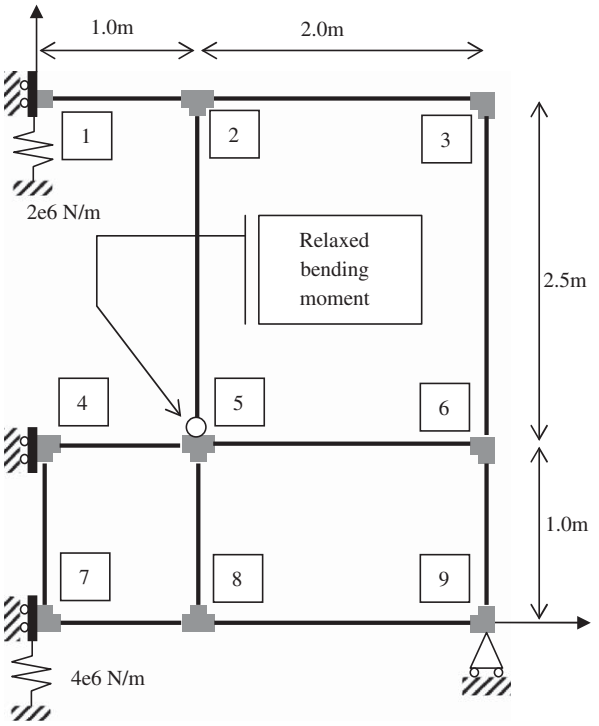

Elements properties						
N.	NODE		Area	Inertia	a_I	a_J
	I	J	$10^{-3}m^2$	$10^{-5}m^4$	m	m
1	1	2	0.75	0.14	0.10	0.10
2	2	3	0.75	0.14	0.10	0.20
3	3	5	1.20	0.82	0.10	0.00
4	4	6	3.50	5.00	0.10	0.00
5	5	5	1.50	3.20	0.10	0.10
6	6	6	1.50	3.20	0.10	0.10
7	7	4	4.00	8.50	0.20	0.20
8	8	5	4.00	8.50	0.20	0.20
9	9	6	4.50	9.00	0.25	0.20
10	7	8	5.00	10.5	0.30	0.30
11	8	9	5.00	10.5	0.30	0.30
b_I and $b_J = 0$ for all elements						

Fig. D4. Cross-section of a ship-like structure.

D.3. Global displacements and loads

To transform the local displacement and loads to the global coordinate system the following standard transformation is used:

$$\underset{6M\times 1}{\mathbf{Q}^{*}(t)} = \underset{6M\times 6M}{\boldsymbol{\phi}_{Q}}\ \boldsymbol{\Theta}\sin(\omega t) \tag{D.16}$$

Natural frequencies (Hz)		
MODE	VIGENE	FEM (1)
	9 Nodes	109 Nodes
1	87.899	86.746
2	115.28	115.29
3	190.17	190.38
4	246.01	245.86
(1) ANSYS : based on consistent mass with rotatory inertia		

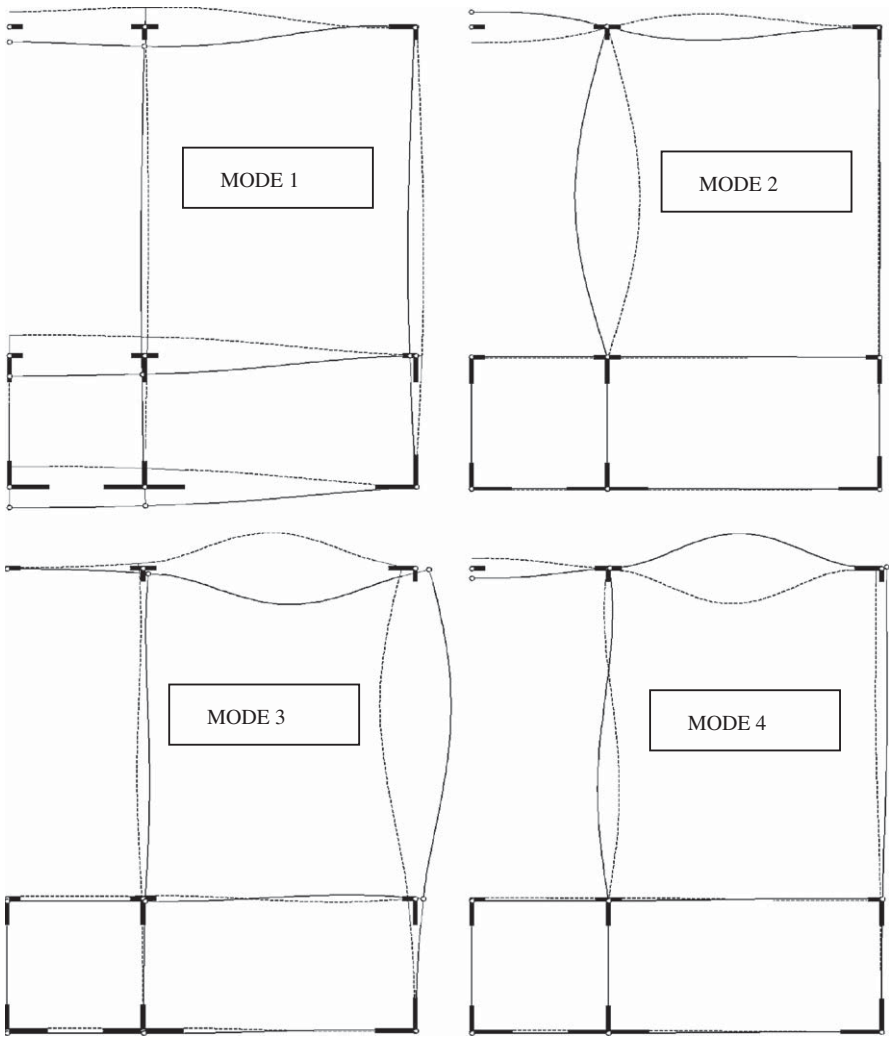

Fig. D5. Natural vibration modes and frequencies for the problem in Fig. D4.

and

$$\underset{6M\times 1}{\mathbf{P}^*(t)} = [\ \underset{6M\times 6M}{\boldsymbol{\phi}_P}\ -\omega^2\ \underset{6M\times 6M}{\boldsymbol{\phi}_{PQ}}\ ]\boldsymbol{\Theta}\sin(\omega t), \tag{D.17}$$

where

$$\boldsymbol{\phi}_Q = \mathrm{diag}[\mathbf{R}_{Qi}\ \ \mathbf{T}_{Qi}\ \ \boldsymbol{\phi}_{Qi}]_{i=1,2,\ldots,M}, \tag{D.18}$$

$$\boldsymbol{\phi}_P = \mathrm{diag}[\mathbf{R}_{Pi}\ \ \mathbf{T}_{Pi}\ \ \boldsymbol{\phi}_{Pi}]_{i=1,2,\ldots,M} \tag{D.19}$$

and

$$\boldsymbol{\phi}_{PQ} = \mathrm{diag}[\mathbf{R}_{Pi}\ \ \mathbf{S}_{Qi}\ \ \boldsymbol{\phi}_{Qi}]_{i=1,2,\ldots,M}, \tag{D.20}$$

with index i being reinstated.

The formulation allows one to assemble the eigenvalue problem from the dynamic stiffness matrix in the same way as discussed in the main section of this paper.

There are quite a few practical problems where the attachment of out of plane particles are important. Consider the problem depicted in Fig. D3, where an equipment rests on a simply supported beam. The equipment has its mass centre out of the beam neutral line and this can be taken into consideration with the formulation described here. This problem presents an exact solution developed in Ref. [21] and further improved in Ref. [22].

The results in Table D1 refer to the configurations depicted in Fig. D3. In model A, the equipment was not yet installed on the beam. In model B, a concentrated mass was added to represent the equipment, but with incorrect flexible spans and with the equipment mass aligned with the beam neutral line. In model C, the beam span supporting the mass was considered rigid. Eccentricity was finally corrected in model D. The results are compared with the ones obtained with the method discussed in Refs. [21,22]. Note that model B, wrongly, is only mass sensitive to the odd modes. Also, the exact solution in Ref. [21,22] cannot be used in model D since it does not consider a concentrated mass off the beam neutral line. In this case, a finite element model was used.

As a final application, consider Fig. D4, which represents the cross-section of a ship-like structure. This problem is particularly attractive here inasmuch as it presents all the features of the linear dynamics of the framed structures so far studied.

The geometry of the various beam elements is also given in Fig. D4, with the frames having standard mild-steel properties, elastic modulus of $E = 200\,\mathrm{GPa}$ and density of $\rho = 7800\,\mathrm{kg/m^3}$.

The first four natural frequencies and mode shapes for this problem are shown in Fig. D5. They are calculated exactly, following the theory here presented, and numerically, via the finite element programme ANSYS when using the consistent mass matrix and rotatory inertia.

References

[1] B. Zhu, A. Leung, Dynamic stiffness for thin-walled structures by power series, *Journal of Zhejiang University* 7 (2006) 1351–1357.
[2] J. Banerjee, Development of an exact dynamic stiffness matrix for free vibration analysis of a twisted Timoshenko beam, *Journal of Sound and Vibration* 270 (2004) 379–401.
[3] J. Banerjee, Dynamic stiffness formulation and its application for a combined beam and two degree-of-freedom system, *Journal of Vibration and Acoustic* 125 (2003) 315–358.
[4] U. Lee, J. Kim, J. Shin, A. Leung, Development of a Wittrick–Williams algorithm for the spectral element model of elastic-piezoelectric two-layer active beams, *International Journal of Mechanical Sciences* 44 (2002) 305–318.
[5] S. Ilanko, F. Williams, Wittrick–Williams algorithm proof of bracketing and convergence theorems for eigenvalues of constrained structures with positive and negative penalty parameters, *International Journal for Numerical Methods in Engineering* 75 (2008) 83–102.
[6] M. Djoudi, D. Kennedy, F. Williams, S. Yuan, K. Ye, Exact substructuring in recursive Newton's method for solving transcendental eigenproblems, *Journal of Sound and Vibration* 280 (2005) 883–902.
[7] F. Williams, M. Djoudi, W. Howson, D. Kennedy, A. Watson, S. Yuan, W. Zhong, Recent transcendental eigensolution advances in structural engineering and other disciplines, *WCCM VI, APCOM'04*, Beijing, China, 2004.
[8] Z. Qi, D. Kennedy, F. Williams, An accurate method for transcendental eigenproblems with a new criterion for eigenfrequencies, *International Journal of Solids and Structures* 41 (2004) 3225–3242.
[9] S. Yuan, K. Ye, F. Williams, Second order mode-finding method in dynamic stiffness matrix method, *Journal of Sound and Vibration* 269 (2004) 589–608.
[10] S. Yuan, K. Te, F. Williams, D. Kennedy, Recursive second order convergence method for natural frequencies and modes when using dynamic stiffness method, *International Journal for Numerical Methods in Engineering* 56 (2003) 1795–1814.
[11] B. Rafezy, W. Howson, Exact natural frequencies of three-dimensional shear-torsion beam with doubly asymmetric cross-section using a two-dimensional approach, *Journal of Sound and Vibration* 295 (2006) 1044–1059.
[12] D. Chen, J. Wu, The exact solutions for the natural frequencies and mode shapes of non-uniform beams with multiple spring-mass systems, *Journal of Sound and Vibration* 255 (2002) 299–322.
[13] K. Ye, F. Williams, Quadratic representation of a nonlinear dynamic stiffness matrix and related eigenvalue problems, *Computer Methods in Applied Mechanics and Engineering* 145 (1997) 313–323.
[14] K. Ye, F. Williams, Bounding properties for eigenvalues of a transcendental dynamic stiffness matrix by using a quadratic matrix pencil, *Journal of Sound and Vibration* 184 (1995) 173–183.
[15] F. Williams, D. Kennedy, M.S. Djoudi, The member stiffness determinant and its uses for the transcendental eigenproblems of structural engineering and other disciplines, *Proceedings of the Royal Society A* 459 (2003) 1001–1019.
[16] F. Williams, D. Kennedy, Derivation of new transcendental member stiffness determinant for vibrating frames, *International Journal of Structural Stability and Dynamics* 3 (2003) 299–305.

[17] F. Williams, D. Kennedy, M.S. Djoudi, Exact determinant for infinite order FEM representation of a Timoshenko beam-column via improved transcendental member stiffness matrices, *International Journal for Numerical Methods in Engineering* 59 (2004) 1355–1371.
[18] R. Clough, J. Panzien, *Dynamics of Structures*, McGraw-Hill, Tokyo, 1975.
[19] K. Bathe, *Finite Elements Procedures*, Prentice-Hall, New Jersey, 1996.
[20] C. Dias, *Computational System for Dynamic Analysis of In-plane Beam Structures—viandi/vigene*, ISBN 978-85-908395-0-7, published online in 〈www.gmsie.usp.br〉.
[21] O. Kopmaz, S. Telli, On the eigenfrequencies of a two-part beam-mass system, *Journal of Sound and Vibration* 252 (2002) 370–383.
[22] S. Ilanko, On the eigenfrequencies of a two-part beam-mass system: Letter to the editor, *Journal of Sound and Vibration* 265 (2003) 909–910.